

1997

Mechanism of iron uptake by cation exchange resins in boiling water reactors used in the nuclear power industry

Sebnem Karakoc
San Jose State University

Follow this and additional works at: https://scholarworks.sjsu.edu/etd_theses

Recommended Citation

Karakoc, Sebnem, "Mechanism of iron uptake by cation exchange resins in boiling water reactors used in the nuclear power industry" (1997). *Master's Theses*. 1504.

DOI: <https://doi.org/10.31979/etd.5t4u-k8x4>

https://scholarworks.sjsu.edu/etd_theses/1504

This Thesis is brought to you for free and open access by the Master's Theses and Graduate Research at SJSU ScholarWorks. It has been accepted for inclusion in Master's Theses by an authorized administrator of SJSU ScholarWorks. For more information, please contact scholarworks@sjsu.edu.

INFORMATION TO USERS

This manuscript has been reproduced from the microfilm master. UMI films the text directly from the original or copy submitted. Thus, some thesis and dissertation copies are in typewriter face, while others may be from any type of computer printer.

The quality of this reproduction is dependent upon the quality of the copy submitted. Broken or indistinct print, colored or poor quality illustrations and photographs, print bleedthrough, substandard margins, and improper alignment can adversely affect reproduction.

In the unlikely event that the author did not send UMI a complete manuscript and there are missing pages, these will be noted. Also, if unauthorized copyright material had to be removed, a note will indicate the deletion.

Oversize materials (e.g., maps, drawings, charts) are reproduced by sectioning the original, beginning at the upper left-hand corner and continuing from left to right in equal sections with small overlaps. Each original is also photographed in one exposure and is included in reduced form at the back of the book.

Photographs included in the original manuscript have been reproduced xerographically in this copy. Higher quality 6" x 9" black and white photographic prints are available for any photographs or illustrations appearing in this copy for an additional charge. Contact UMI directly to order.

UMI

A Bell & Howell Information Company
300 North Zeeb Road, Ann Arbor MI 48106-1346 USA
313/761-4700 800/521-0600

MECHANISM OF IRON UPTAKE BY CATION EXCHANGE RESINS
IN BOILING WATER REACTORS USED IN THE NUCLEAR POWER INDUSTRY

A Thesis

Presented to

The Faculty of the Department of Chemical Engineering

San Jose State University

In Partial Fulfillment

of the Requirements for the Degree

Master of Science

by

Sebnem Karakoc

August 1997

UMI Number: 1386205

UMI Microform 1386205
Copyright 1997, by UMI Company. All rights reserved.

**This microform edition is protected against unauthorized
copying under Title 17, United States Code.**

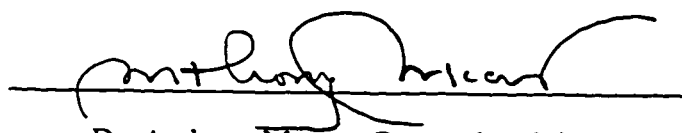
UMI
300 North Zeeb Road
Ann Arbor, MI 48103

©1997


Sebnem Karakoc

ALL RIGHTS RESERVED

APPROVED FOR THE DEPARTMENT OF CHEMICAL ENGINEERING



Dr. Anthony Muscat, Research Advisor

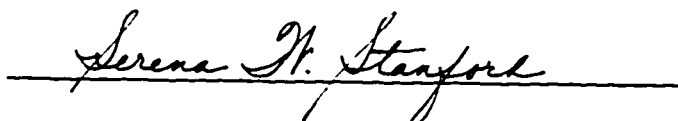


Dr. Paul Frattini, Committee Chairperson



Dr. Leon Yengoyan, Committee Member

APPROVED FOR THE UNIVERSITY



ABSTRACT

MECHANISM OF IRON UPTAKE BY CATION EXCHANGE RESINS IN BOILING WATER REACTORS USED IN THE NUCLEAR POWER INDUSTRY

by Sebnem Karakoc

Styrene based divinyl-benzene crosslinked (DVB) strongly acidic cation exchange resins of 6 % and 10 % crosslink density were packed in mixed beds and investigated for iron uptake in a laboratory scale flow loop apparatus. Resins were exposed to dilute suspensions of submicron particulate iron oxides in high purity water for periods of continuous flow up to 120 hours.

Two forms of iron uptake were observed. The first form, surface iron, was removed by sonicating the cation resins in nanopure water using a laboratory scale ultrasonic cleaner. The second form, matrix diffused iron, was extracted by sonicating the resins in heated H_2SO_4 .

The amount of matrix diffused iron was approximately three times higher in 6 % DVB crosslinked cation resins than in 10 % DVB crosslinked resins. The results demonstrate that iron from a particulate source diffused into the resin matrix and was bound there.

ACKNOWLEDGMENTS

I would like to thank my advising professor, Dr. Anthony Muscat, for his valuable guidance, support and encouragement during this research study. I would like to thank thesis committee chairperson, Dr. Paul Frattini and thesis committee member, Dr. Leon Yengoyan, for their guidance and support through this project. Their input to this study and the use of their laboratory facilities proved invaluable during this research.

I recognize Louis Lou and Mary Silva for their technical support on this project. They each played a pivotal role in establishing experimental analysis and evaluating system parameters.

I would like to thank my husband, Ufuk Karaaslan, for his patience, ideas and support during this study.

I also acknowledge the San Jose State University Foundation for financial support of this project in the form of research assistantships.

Finally, I am grateful to my parents and my sister due to their patience, assistance and encouragement during this study.

TABLE OF CONTENTS

	Page
ABSTRACT	iv
ACKNOWLEDGMENTS	v
TABLE OF CONTENTS	vi
LISTS OF TABLES	viii
LISTS OF FIGURES	ix
CHAPTER 1. INTRODUCTION AND BACKGROUND	1
1.1. Introduction	1
1.2. Background	2
1.3. Operation of a Boiling Water Reactor	3
1.4. Effectiveness of Full Flow Polishers	3
1.5. Maintenance of Full Flow Polishers	4
1.6. Risks Associated With Corrosion Product Particle Release	5
1.7. Iron Control Techniques in Condensate Cleanup Systems	6
1.8. Iron Removal Optimization	6
1.9. Technical and Economical Justification for Iron Removal	7
CHAPTER 2. LITERATURE REVIEW	8
2.1. Literature Trends	8
2.2. Swedish Studies	8
2.2.1. The Origin of Corrosion Product Particles	8
2.2.2. Determination of Particle Size	9
2.2.3. Phases	9
2.2.4. Morphology	9
2.2.5. Surface Charge	10
2.2.6. Particle Formation	11
2.3. Japanese Studies	12
2.3.1. Forms of Uptake	12

2.3.2. Aging Effect on Crud Removal	Page 14
CHAPTER 3. MATERIALS AND METHODS	16
3.1. Introduction	16
3.2. Research Hypothesis	16
3.3. Experimental Design and Apparatus	17
3.4. Experimental Procedure	19
3.5. Analytical Method	21
CHAPTER 4. EXPERIMENTAL RESULTS	24
4.1. Introduction	24
4.2. S2 (6 % DVB Crosslinked) Experimental Matrix	24
4.2.1. Fe ₂ O ₃ Runs With S2	31
4.2.2. Fe ₃ O ₄ Runs With S2	31
4.2.3. Mixed Oxide Run With S2	32
4.3. H1 (10 % DVB Crosslinked) Experimental Matrix	35
4.4. Saturated Amount of Ferric Ion Loading on S2 and H1	36
CHAPTER 5. DISCUSSION	38
CHAPTER 6. CONCLUSION	46
REFERENCES	47
APPENDICES	49
Appendix A: UV/vis Spectrophotometer Technique	49
Appendix B: Fe ³⁺ Determination Method	51
Appendix C: Preparation of An Iron Oxide Solution Suspension	53
Appendix D: Experimental Run Time Calculations	55
Appendix E: Flow Loop Mass Balance	56
Appendix F: Power Determination of Branson 5210 Ultrasonic Cleaner	58

LISTS OF TABLES

	Page
Table 2.1. Properties of Virgin and Aged Cation Resins.	14
Table 3.2. Properties of The Iron Oxide Powders.	19
Table 3.3. Characteristics of Experimental Cation Exchange Resins.	20
Table 3.4. Standard Calibration Curve Data.	22
Table 3.5. Investigation Methodology of The Cation Exchange Resins.	22
Table 4.1. S2 (6 % DVB crosslinked) Experimental Matrix Variables.	25
Table 4.2. The Surface Iron Data, Fe ₂ O ₃ -S2 #3.	26
Table 4.3. The Matrix Diffused Data, Fe ₂ O ₃ -S2 #3.	28
Table 4.4. S2 Experimental Matrix Data.	30
Table 4.5. Mixed Oxide Weight Percentages.	33
Table 4.6. Mixed Oxide Data, S2.	33
Table 4.7. H1 (10 % DVB crosslinked) Experimental Matrix Variables.	35
Table 4.8. H1 Experimental Matrix Data	35
Table 4.9. Fe ³⁺ Saturation Data.	37
Table 5.1. Percentage of MDI over TIE, SI; S2.	38
Table 5.2. Percentage of MDI over TIE, SI; H1.	40
Table 5.3. Percentage of MDI over SI; S2 and H1	42
Table 5.4. Crud removal results reported by Yushikawa <i>et al.</i> (1989)	45

LISTS OF FIGURES

	Page
Figure 3.1. Experimental Apparatus.	17
Figure 4.1. Surface Iron Plateau, Fe_2O_3 -S2 #3.	26
Figure 4.2. Exponential Fit Curve For The Amount of Surface Iron For Experiment, Fe_2O_3 -S2 #3.	27
Figure 4.3. Matrix Diffused Iron Plateau, Fe_2O_3 -S2 #3.	28
Figure 4.4. Exponential Fit Curve For The Amount of Matrix diffused Iron For Experiment, Fe_2O_3 -S2 #3.	29
Figure 4.5. Accumulated Amount of Iron and Total Iron Exposure, S2 matrix.	30
Figure 4.6. Accumulated Amount of Iron and Total Iron Exposure, mixed oxides.	34
Figure 4.7. Accumulated Amount of Iron and Total Iron Exposure, H1 matrix.	36
Figure 5.1. % Matrix Diffused Iron Over Total Iron Exposure, S2.	39
Figure 5.2. % Matrix Diffused Iron Over Surface Iron, S2.	39
Figure 5.3. % Matrix Diffused Iron Over Total Iron Exposure, H1.	40
Figure 5.4. % Matrix Diffused Iron Over Surface Iron, H1.	41
Figure 5.5. % Matrix Diffused Iron Over Surface Iron, all Fe_2O_3 runs.	42
Figure 5.6. % Matrix Diffused Iron Over Surface Iron, all Fe_3O_4 runs.	43

CHAPTER 1. INTRODUCTION AND BACKGROUND

1.1. Introduction

The corrosion product particles formed in boiling water reactor coolant systems cause a wide range of problems due to reduced heat transfer and transportation of radioactivity. Current Electric Power Research Institute (EPRI) guidelines call for an optimal feedwater iron level of 0.5 to 1.5 ppb.

It is of prime interest to reduce the corrosion product particles using already available technologies such as deep bed condensate polishers or dual cleanup systems. While installation of prefilter systems is an option, it is more economical for plants with naked deep beds to find an improved resin for use in existing systems.

We used styrene based divinylbenzene (DVB) crosslinked and strongly sulfonated cation exchange resins in order to understand the filtration form of particulate iron in a mixed bed. The hypothesis is that the acidic environment provided by the sulfonated groups would cause particulate iron to dissolve locally and form chemical interactions with the sulfonated groups in the pores of the cation exchange resins.

To investigate the reasonableness of this hypothesis, a laboratory scale flow loop apparatus was designed and suspensions of submicron particulate iron solutions were fed to the cation exchange resins in a mixed bed. Six percent (6 %) and ten percent (10 %) DVB crosslinked cation exchange resins were used in a series of experiments. Two forms of iron uptake were observed by the cation exchange resins. The first form, called surface

iron, was obtained by sonicating the cation resins in water and by analyzing concentrations of the sonicated solutions using a UV/vis spectrophotometer. The second form called matrix diffused iron was extracted by sonicating the already sonicated cation resins in hot H_2SO_4 . Concentrations of the sonicated acid solutions were again determined using the UV/vis spectrophotometer.

The results of the experiments showed that 15 to 25 % of the total amount of accumulated iron was contributed by the second form, thus proving the existence of matrix diffused iron.

1.2. Background

Core components in steam generation systems can undergo serious material degradation by a variety of corrosion-related phenomena. These occurrences are largely controlled by boiler water chemistry, which is strongly impacted by the performance of the mixed bed ion exchange units called Condensate Polishers. In nuclear power industry boiling water reactor (BWR) systems, the condensed water stream passes through a condensate polisher system which is packed with anion and cation exchange resin to remove soluble and insoluble impurities.

Ion exchange resins are bead like polymeric matrixes with an affinity for particular ions. Salmon *et al.* (1959) explained the polymerization of the styrene based sulfonic acid cation exchange resins; styrene is first polymerized with divinylbenzene in suspension and cured. The styrene-divinylbenzene copolymer is then sulfonated with sulfuric acid. Sulfonic acid groups will exchange hydrogen ions for any cation they

encounter. Similarly, anion exchange resins, made of styrene and divinyl-benzene containing quaternary ammonium groups, will exchange a hydroxyl ion for any anion.

1.3. Operation of a Boiling Water Reactor (BWR)

A boiling water reactor (BWR) is a direct cycle system in which water passes the core acting as both a moderator and a coolant. A portion of the coolant evaporates and enters the turbine as steam. The condensed steam is collected in a hot well located below the condenser cooling tubes. Flow from turbine extraction lines also eventually returns to the hotwell, picking up corrosion products in feed water heaters. The full flow of condensate passes through a mixed bed ion exchange unit (full flow polisher) in order to remove impurities.

1.4. Effectiveness of Full Flow Polisher

Polishers are effective in preventing condenser leakage impurities from reaching BWR Vessel Internals and also provide adequate time for a corrective action, including shutdown if necessary

Equally important to the reactor water chemistry is the necessity of preventing ion exchange resin fragments from entering the reactor core where complete thermal degradation can take place and produce increased reactor water conductivity. Resin fragments are routinely produced by the mechanical compression, agitation, abrasion and hydraulic shocking involved in the normal operation, transport, and cleaning of the deep bed ion exchange resins. Significant amounts of these fragments, typically referred to as

“fines” will be small enough to pass through the ion exchangers and subsequently enter the reactor feedwater. Cation resin fines entering the reactor will produce an increased concentration of soluble sulfates. To avoid this increase, the external cleaning process utilized for insoluble corrosion product removal from the ion exchange resins must also be capable of effectively removing any resin fines present in the resin mass.

By reducing the amount of insoluble iron entering deep bed demineralizers, the life time and performance of the resins will be improved substantially. Reduction of iron fouling will improve the ion exchange performance and will reduce periodic cleaning of the resins by ultrasonic means or by backwashing. Also, since the resin bed will not be disturbed or mixed by these operations, the usable ion exchange capacity will be increased by maintaining the low ionic loading at the bed outlet.

1.5. Maintenance of a Full Flow Condensate Polisher

In the early years of BWR operation, it was thought that under normal conditions oxygenated water with low conductivity would be sufficient to guarantee the 40 year design lifetime for plant components. However, poor removal of particulate corrosion products (especially iron oxides) from the condensate demineralizer inlet is one of the major problems in BWR systems today.

In BWR, the mixed bed ion exchange units not only provide protection from ionic contaminants, but also remove insoluble corrosion products by filtration/ adsorption. These insoluble corrosion product particles removed by the ion exchanger units must be

periodically cleaned from the resin bed by some process external to the BWR's primary water loop.

Mixed bed ion exchange units in BWRs are periodically removed from service to clean any accumulated insoluble corrosion products and resin fines. Some of the conditions that necessitate bed cleaning are excessive differential pressure across the ion exchange bed, increased reactor water conductivity and high concentrations of corrosion product particles in the reactor feedwater.

1.6. Risks Associated with Corrosion Product Particle Release

Work by Ishigure *et al.* (1983) explained the risks associated with iron release to the feed water systems in nuclear power reactors. The majority of the iron entering the reactor vessel by way of the feed water system deposits on fuel cladding surfaces where it absorbs cobalt and other soluble reactor water impurities. While on the cladding surfaces, these metal impurities become neutron activated and some fraction are subsequently released to the reactor water as soluble or insoluble radioactive isotopes. By way of the reactor water, they are transported throughout the primary system and accumulated on piping and equipment surfaces resulting in reactor building general area dose rates. By reducing iron input to the primary system, the fuel surface inventory of both iron and non-radioactive cobalt (Co-59) absorbed by the iron is reduced, thus reducing the source of activated Co-60.

Reduction of iron input into the BWR primary system has long been recognized by nuclear power plants as an important first step in the reduction of radiation fields and occupational exposure.

Because of these concerns, current Electric Power Research Institute (EPRI-1996) guidelines call for an optimal feed water iron target of 0.5 to 1.5 ppb.

1.7. Iron Control Techniques in Condensate Cleanup Systems

EPRI *et al.* (1993) reported two types of control techniques in condensate cleanup systems. The first one was using deep beds only. They were cost effective; however, iron removal rate was 70 %. The second was hollow fibers and fiber matrix filters. They were placed upstream of existing deep bed condensate polishers, and achieved iron removal rate of 95 % and greater. However, filters successfully operated in Japan at lower temperatures might not perform as well at higher temperatures in the United States and operation and maintenance costs have to be justified.

1.8. Iron Removal Optimization

Reduction of target iron level with available technologies (e.g. replacement or material improvements, dual condensate cleanup systems, low crosslinked resins) is highly desirable.

It has become clear that conventional deep bed resins are largely incapable of meeting target feedwater iron concentrations. While installation of prefilter systems is an

option, it would be more economical for plants with naked deep beds to find an improved resin for use in existing systems.

1.9. Technical and Economical Justification for Iron Removal

EPRI *et al.* (1993) summarized the net effect of reduced iron input to the deep bed demineralizers. They were improved feedwater quality, reduced liquid and solid radioactive waste, lower radiation fields, reduction in depleted zinc addition requirement, and reduced operation and maintenance costs.

CHAPTER 2. LITERATURE REVIEW

2.1. Literature Trends

This literature review summarizes the previous studies conducted on the origin of corrosion product particles, the filtration process of corrosion product particles by ion exchange resins and factors involved in the filtration process.

Most of the studies on corrosion product particles and water chemistry in BWRs were conducted by Swedish, Japanese and American researchers. Swedish researchers studied the origin and phase of the corrosion products. Japanese researchers focused on corrosion particle up-take by ion-exchange resins. American researchers *in situ* studied the uptake of condensate stream corrosion product particles by ion exchange resins at different power plants in the US.

2.2. Swedish Studies

2.2.1. The Origin of Corrosion Product Particles

Most plants in Sweden were designed with the main part of the turbine made of carbon steel having more than 95 % iron and not having high corrosion resistance. Therefore plants required extensive material upgrading. Later the high pressure steam extraction lines were replaced with type 304 SS which has higher resistance to corrosion (Hermansson *et al.*, 1992).

Hermansson *et al.* (1992) identified the first anodic step of the corrosion product formation as $\text{Fe} = \text{Fe}^{2+} + 2\text{e}^-$.

Persson and Reinvald *et al.* (1992) analyzed the particle size, phases and morphology of the corrosion particles using surface analysis equipment such as Mossbauer Spectroscopy, Scanning Electron Microscopy (SEM), Atomic Absorption Spectrometer, X- Ray Diffraction

2.2.2. Determination of Particle Size

Using a combination of Mossbauer Spectroscopy and the SEM method, they found that 75% of the particles have a diameter less than 0.1 μ .

2.2.3. Phases

Work by Hermansson *et al.* (1992) showed different corrosion product particle phases using X-ray diffraction. The most common phases were magnetite, Fe_3O_4 ; hematite, Fe_2O_3 ; goethite, $\alpha\text{-FeO(OH)}$; and lepidocrocite, $\gamma\text{-FeO(OH)}$.

2.2.4. Morphology

Corrosion product particles were by Hermansson *et al.* (1994) in the following forms:

1. Small individual particles with a crystalline appearance.
2. Small individual particles with an amorphous appearance.
3. Agglomerated aggregates composed of a varying number of small crystalline or amorphous particles.
4. Fiber like particles of unknown origin and composition.

2.2.5. Surface Charge

Since surface charge of the particles is directly related to zeta potential, the zeta potential was determined by recording the electrophoretic mobility of particles in water samples (Hermansson *et al.*, Persson *et al.*, Reinvall *et al.*, 1992). The zeta potential of an iron particle was strongly dependent on the pH of the water medium that carried the particle. Work by Hermansson *et al.* (1992) showed that there was a large scatter in the zeta potential readings recorded at the same pH value. This effect was due to the presence of particles with different surface charges which gave a range of zeta potential values at a given pH. Reinvall *et al.* (1992) observed that the zeta potential of an iron particle was positive at low pH and negative at high pH. Most of the corrosion product particles had zeta potentials in the range of -30 to -40 mV at a pH of 7. With the process of crystallization and approach toward equilibrium, the number of chemically active groups such as $\text{Fe-O}^-\text{H}^-$ on the surface decreased as the specific surface area of the particles became smaller. The dependence of the zeta potential on changes in bulk pH thus became smaller as the particle became bigger and more crystalline. Because most of the particles in condensate streams have an amorphous structure, the zeta potential depends strongly on the concentrations of these particles.

The hematite particles had positive charges at $\text{pH} < 8$, the point of zero charge (PZC) occurred approximately at a solution pH of 8 for hematite, and at $\text{pH} > 8$ the hematite particles had negative surface charges. On the other hand, the cation resins had negative charges over the entire pH range. The electrokinetic interactions were very

strong at $\text{pH} < 8$, since they had opposite surface charges. On the other hand, at $\text{pH} > 8$ the electrokinetic interactions were repulsive between the particles and the cation resins because of the same surface charges

2.2.6. Particle Formation

Corrosion product particles formed in the cold systems, such as condensers, were either in the form of magnetite or, as phase transitions were slow, in the form of amorphous Fe(III) particles. In the hot systems, such as preheater drains, phase transitions were favored, and as a result, crystalline Fe(III) phases were more commonly observed.

2.3. Japanese Studies

In Japan, the latest BWR plants were furnished with a condensate filter that was upstream of deep the bed type condensate demineralizer. Using the combination of the two filtration systems, removal efficiencies of corrosion product particles are in the range of 97-99 % in the Japanese plants. However, attention was paid to the plants with only deep bed filtration systems. Studies were focused on the improvement of iron-uptake and modification of the conventional type ion-exchange resins.

In Japan, the bulk of the resins used in BWR condensate polishers were 8 % crosslinked gel resins. Work by Inami and Nagao *et al.* (1989) indicated that a lower crosslinked cation resin would result in lower effluent particulate iron values. Iron particulate values of less than 1 ppb. were achieved by changing the cation resin to a special 6 % crosslinked material. Nagao *et al.* (1989) implied that the resin had a certain surface characteristic which improved its iron particulate removal efficiency.

Based on filtration theory, in a BWR environment the cation resin is the prime adsorbent for the removal of iron. In addition, greater the resin surface area will result in better iron removal.

2.3.1. Form of Uptake

Mixed resin test column was installed in an actual Japanese BWR plant to study iron uptake. Captured iron called as “crud” was classified and analyzed by Kawazu *et al.*, Hemmi *et al.*, Yoshikawa *et al.*, (1989).

The anions were separated from the cation resins by fluidizing the test column. Light density anions floated to the top of the column and were collected. The cations were kept in the column and loosely deposited iron between the water and resin surface was torn off by air scrubbing and backwashing the column. The collected solution was filtered and the obtained iron was called loosely captured iron. The second form of iron was obtained by ultrasonic cleaning of the same cation resins. The solution was filtered and the form of iron was called tightly formed. The final form of iron was obtained by extracting acid over already two times treated cation resins. The final form was called incorporated iron into resin beads. Following schematic is a representation of the analysis methodology.

RESIN SAMPLE ↓			
⇒ Scrubbing	⇒ Backwash water	⇒ Filtration	⇒ Loosely captured iron
⇒ Ultrasonic cleaning	⇒ Waste water	⇒ Filtration	⇒ Tightly captured iron
⇒ Resin cleaned	⇒ Acid extraction	⇒ Filtration	⇒ Incorporated Iron

Among the particle uptake forms, incorporated iron played the most important role because this was the rate determining step of the removal process. Kawazu *et al.* (1989) explained incorporation may have happened because iron was soluble under acidic environments as in cation resin pores. The rate of incorporation was faster when the resin surface was more acidic or the micropore size (specific surface area) was larger.

2.3.2. Aging Effect on Crud Removal

Mixed resin column tests performed in Japanese BWRs showed that there was a relation between crud removal efficiency and aged (used) deep bed resins. This phenomenon was called “aging effect”.

The important steps in the crud removal mechanism of cation resins were adsorption and dissolution of crud on the resin surface. Table 2.1 shows some important properties of the virgin and aged cation resins. The water retention and specific surface area were higher in aged one compared to virgin resin. Increased water retention caused by decrosslinking of the cation resins made diffusion of crud faster into the pores.

Table 2.1. Properties of virgin and aged cation resins.

PROPERTIES	CONVENTIONAL GEL RESIN	
	VIRGIN	AGED
Water Retention (%)	55	56-58
Potential (mV)	-37	-49
pH	1.7	1.5
Specific Surface Area (m/g-dry resin)	0.02	0.03

The zeta potential of the resin played a very important role on the iron removal. When the zeta potential of the resin was more negative, the surface charge density of the resin was also more negative. Negative surface charge density made the rate of dissolution of crud faster in the pores of the cation exchange resins.

CHAPTER 3. MATERIALS AND METHODS

3.1. Introduction

The purpose of this study was to determine the filtration form of iron oxides in a neutral mixed bed. Particulate iron oxide solutions were fed into the mixed bed at 300 ppb. concentration ranges at a nominal flow rate of 150 ml./min for approximately 120 hours. Strongly acidic cation exchange resins prepared by the sulfonation of crosslinked polystyrene were investigated for the filtration (iron uptake).

3.2. Research Hypothesis

Particulate iron loaded cation exchange resins were studied to determine whether iron would stay in the form of particulate iron or whether dissolution of iron would occur in the vicinity of the sulfonated groups having a low pH range of 3 to 3.5.

Work by Yoshikawa *et al.* (1989) suggested that fractions of the iron onto the cation resins were identified as in the forms of lightly, tightly bounded and incorporated iron. Determination of lightly and tightly bounded iron was done by back-washing and ultrasonic cleaning of the cation resins. However, incorporated iron was determined by only chemical extraction using HCL or H₂SO₄. He hypothesized that the lower pH range obtained from sulfonated groups in the pores of a cation exchange resin may produce incorporated iron with a chemical bond between Fe³⁺ and SO₃⁻.

In order to determine the filtration form of particle iron by cation exchange resins in a mixed bed, a flow loop apparatus was designed. Filtration experiments were performed on 6 % and 10 % DVB crosslinked cation exchange resins using only particle iron

identified as magnetite, Fe_3O_4 ; hematite, Fe_2O_3 ; goethite, $\alpha\text{-FeO(OH)}$; and epidocrocite, $\gamma\text{-FeO(OH)}$.

3.3. Experimental Design and Apparatus

The experimental apparatus shown in Figure 3.1 was used to perform filtration experiments for iron removal.

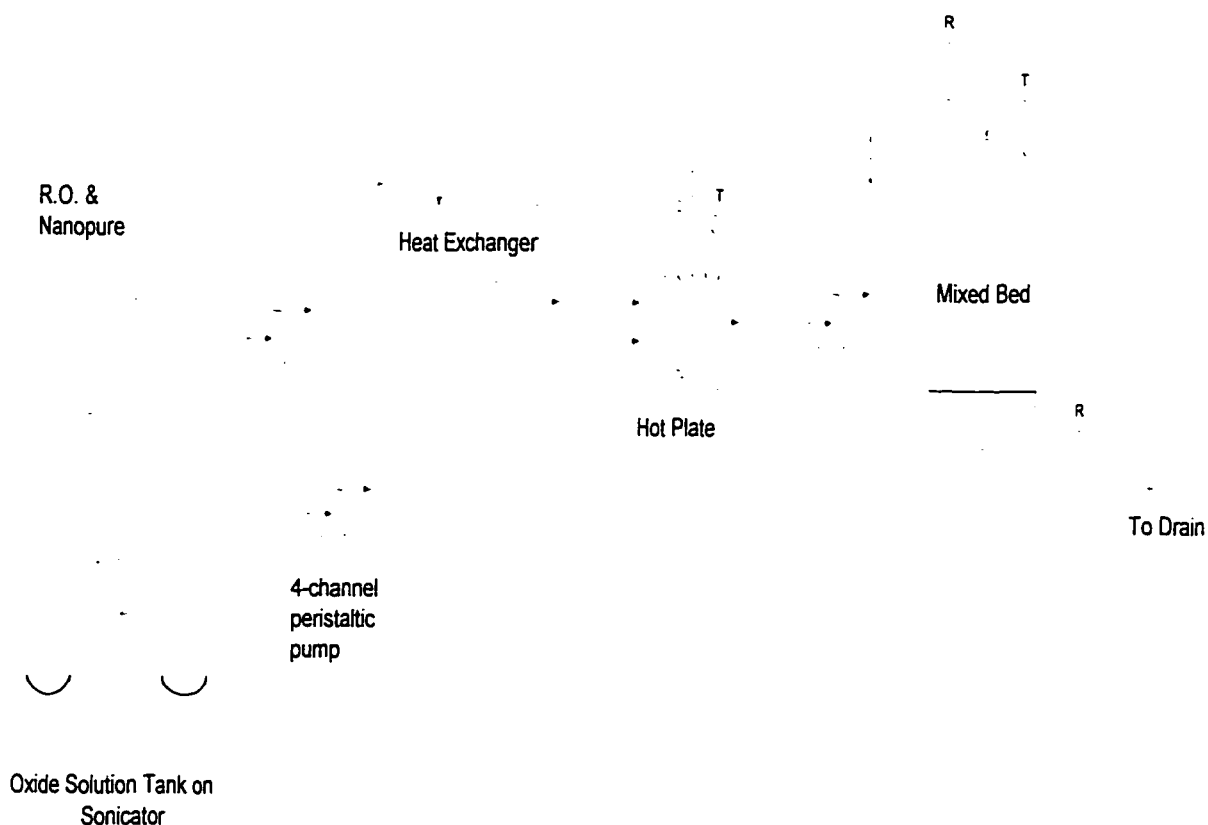


Figure 3.1. Experimental apparatus.

Fundamental equipment is listed below:

1. Continuous water supply (a nominal flow rate of 150 ml./min.) to the apparatus was provided from a Reverse Osmosis system connected to a Nanopure system.
2. Chemical resistance classification charts were used to select proper tubing and piping material. Mainly polyethylene and polypropylene were used.
3. Particle iron loaded solution concentration to the mixed bed was kept in the range of 300 ppb. To achieve this specified dilution limit, very large containers were needed. Both economical and space considerations lead us to another configuration of the apparatus. Iron solution with a higher concentration (in the range of ppm) was prepared in a 4000 ml volumetric flask, passed through a 4-channel very precise Dynamix Peristaltic Pump Model RP-1 with a flow rate of 3.6 ml/min., combined with the main water supply at 150 ml/min. nominal flow rate and fed into the mixed bed at 300 ppb.
4. Conductivity measurements were essential parts of the apparatus in order to make sure a pH range of 7 was achieved. Barnstead PM-510 Purity Meter/Controller and Barnstead threaded in-line cells E 3420 were installed with a range selector switch to read a resistivity range from 0 to 20 M Ω - both from top and bottom of the mixed bed.
5. Teflon coated K-type thermocouples with miniconnectors were used first into the mixing reservoir, second at the top of the mixed bed and finally at the bottom of the mixed bed.
6. In order to keep iron solution in suspension, a Branson 5210 ultrasonic cleaner was used.
7. A water bath and a heat exchanger were used to heat up the solution to 55C°.

3.4. Experimental Procedure

Filtration of corrosion product particles, iron oxides, was studied in a continuous flow loop. Four different types of iron oxide were used with two different percentage DVB crosslinked cation exchange resins. Table 2. is a representation of the properties of the iron oxide powders

Most of the full flow deep bed condensate polishing systems in the nuclear power plants use 50 gpm/ft² and operate at 55 C°. In this study, a nominal flow rate of 150 ml/min. was the operational flow rate through a laboratory scale Reverse Osmosis and Nanopure system. Each experimental run lasted 120 hours (5 days) with a nominal flow rate of 0.734 gpm/ft². Iron oxide powders were

Table 3.2. Properties of the iron oxide powders.

Iron (II, III) oxide, Puratronic, 99.997 % (metals basis), Fe ₃ O ₄
Iron (III) oxide, Puratronic, 99.99 % (metal basis), Ferrite Grade, Fe ₂ O ₃
Iron (III) hydroxide, gamma and alfa, 99 %

Initially 0.005 weight percentage was chosen for iron solution preparation. It was detected that most of the particle iron was not suspendible in the solution even with the help of a mixer and a sonicator. However, lowering the weight percentage to 0.00125, desirable suspensions were achieved with the help of a sonicator. Use of lower weight percentage was based upon reports by Kataby *et al.* (1995) and Koltypin (1995).

For each experimental run, 0.05 gr. of iron oxide was weighted into a 4000 ml volumetric flask and diluted to the mark. Total volume of iron solution over each experimental run was 25960 ml. Each 4000 ml. solution first was stirred in a mixer

approximately 12 to 24 hours. Then it was sonicated in 99 minutes time intervals to keep iron particles suspended in the solution.

Mixed bed preparation was based on the wet volume of the exchange resins. Five ml of each resin was used during the preparation with a ratio of 1:1 (anion /cation). Temperature, particle size range, poly dispersity and resistivity were recorded daily. The resistivity probes placed at the top and the bottom of the mixed bed continuously checked the purity of the water and they never read lower than 12 MΩ-cm. Therefore, even though the exchange capacity of the anion resins was lower than the cation resins, dissolution of the iron oxides (lower pH caused by acidic cation exchange resins) did not happen while running through the mixed bed in the flow loop.

Four different iron oxide solutions were used in S2 (6 % DVB crosslinked) and in H1 (10 % DVB crosslinked) experimental matrixes. Sample resins provided by Electric Power Research Institute performed in the actual Condensate Polisher's. Some of the characteristics of the samples are summarized in the Table 3.3.

Table 3.3. Characteristics of Experimental Cation Exchange Resins.

% Crosslink	Origin, lot #	Capacity (meq/ml)	Water Retention Capacity % (H ⁺)	Average Diameter, μm	Type
10	Hope Creek 1 1 BD 0437	2.0	49	752	Gel
6	Susquhenna 2 1479	1.6	62	546	Gel

3.5. Analytical Method

Experiments were performed in a continuous flow loop using a neutral mixed bed packed with ion exchange resins. Strongly acidic styrene DVB crosslinked cation exchange resins were sought for the adsorption/ filtration of iron oxides.

Both the superficial washes for surface iron and acid washes for matrix diffused iron were done on the cation exchange resins to determine the concentration of the ferric ion (Fe^{3+}) using a UV/vis.

Iron determination method and the standard calibration curve were developed with the help of Dr. Leon Yengoyan in the Chemistry Department at SJSU and Dr. Paul Frattini at Electric Power Research Institute (EPRI). Preparation of iron standards and determination method of iron in natural water supplies are explained in the Appendix B.

After each experimental run, cation exchange resins have to be separated from the anions. Since anion exchange resins had lighter densities than the cation exchange resins, hydraulic separation and density separation were enhanced by the differences in anion and cation resin densities. The mixed bed was backwashed and anions in the fluidized bed floated to the top and a pipette placed into the top of the mixed bed collected the upcoming anion resins from the cation resins. Iron determination methodology is described in Table 3.5.

A standard calibration curve was produced before each experiment was performed. Known concentrations of the iron solutions were run through the

spectrophotometer. Absorbance at 508 nm versus concentration in micrograms / milliliter (μ grams/ml) are shown in Table 3.4 for the standard calibration curve.

Table 3.4. Standard calibration curve data.

Absorbance at 508 nm	Concentration, microgram/ml
0.000	0 (water blank)
0.098	0.5
0.197	1.0
0.395	2.0
0.491	2.5
0.981	5.0

Table 3.5. Investigation methodology of the cation exchange resins.

Mixed bed: Ratio of anion resins to cation resins \Rightarrow 1:1, volume of 5 ml /5 ml	
Cation (sample)	Anion (removed)
CATION	
↓	
Wash Water \Rightarrow Iron Analysis	Sample
SAMPLE	
Surface iron (Superficial wash) analysis:	
<ul style="list-style-type: none"> The cation resins were sonicated in fresh 100 ml nanopure water in 99 minute time intervals, sonicated solutions were analyzed until 1 % of the first concentration was achieved. 	
Cation resins then were put under vacuum (2 to 3 days) until a dry weight base was obtained.	
One gram of dry cation resins was weighted for acid wash analysis, rest of it was saved.	
Matrix Diffused Iron (Acid wash) analysis:	
<ul style="list-style-type: none"> Sonicator was set up at 55 C° to heat 6M H₂SO₄ . 15 ml hot acid was added to 1- gram of the cation resins and sonicated in 99 minute time intervals. Sonicated hot acid solutions were analyzed until 1 % of the first concentration was achieved. 	
Concentration readings were obtained using a UV/vis spectroscopy. UV/vis analysis procedure is explained in Appendix A.	

The sample cation resins were placed in a volumetric flask containing 100 ml nanopure water and sonicated for 99 minutes. Fifteen (15.0) ml of this solution was kept in hot steam approximately for 5 minutes to dissolve particle iron. After the hot steam treatment, the color of the iron solution became clear. This solution was placed in a 100 ml volumetric flask. One (1.0) ml of hydroxylamine hydrochloride (10 grams of $\text{H}_2\text{NOH.HCL}$ is dissolved in about 100 ml of deionized water), 10 ml of sodium acetate (166 grams of $\text{NaOAc.3H}_2\text{O}$ is dissolved in 1000 ml of deionized water) and 10 ml of orthophenantroline solution (0.1 grams of orthophenantroline monohydrate is dissolved in 100 ml deionized water) were also added to the 100 ml volumetric flask and diluted to 100 ml mark. First the standards then the iron containing solution were run through the spectrophotometer in order to determine both the standard iron solution concentration and the concentration of the sonicated solution. Sonication of the cation resins was repeated with 100 ml fresh nanopure water and same analysis was performed until 1 % of the first concentration reading was obtained. Accumulated amount of the iron was calculated and called surface iron. Cation resins were put under vacuum approximately three days to obtain dry weight. One (1.0) gram of the dry cation resin was put in 15 ml heated 6 N H_2SO_4 acid and sonicated another 99 minutes. Sonicated acid solution was analyzed exactly the same as surface iron. Sonication was repeated with fresh 15 ml heated 6 N H_2SO_4 acid and was terminated when 1 % of the first acid solution concentration was obtained. Accumulated amount of acid extracted iron was calculated and called matrix diffused iron.

CHAPTER 4. EXPERIMENTAL RESULTS

4.1. Introduction

Six percent (6 %) styrene DVB crosslinked cation exchange resins (Susquehanna-2: S2) and ten percent (10 %) styrene DVB crosslinked cation exchange resins (Hope Creek-1: H1) were used with four different iron oxide solutions (magnetite, Fe_3O_4 ; hematite, Fe_2O_3 ; goethite, $\alpha\text{-FeO(OH)}$; and lepidocrocite, $\gamma\text{-FeO(OH)}$). Some of the experiments were repeated to check repeatability of results. The names of the experiments that appear in the following pages are obtained by combining the solution name, cation sample name and the repetition number. For example Fe_2O_3 -S2 #2 refers to the second experiment done using the S2 sample in the Fe_2O_3 solution.

For all the experimental runs, Standard Basic (SBR-C, Dow product) 10 % DVB crosslinked anion exchange resins were used while preparing the mixed bed. System parameters such as temperature, resistivity and particle size of the solutions were monitored daily.

4.2. S2 (6 % DVB Crosslinked) Experimental Matrix

Six experimental runs were performed using S2 sample which was identified as DOW XUS43550 stabilized 6 % DVB crosslinked cation exchange resin. Each series of data was obtained when 120 hours continuous run was over. To analyze the cation resin performance, the anions were separated from the cation resins as described in section 3.5. Table 4.1 lists experimental variables involved in the S2 (6 % DVB Crosslinked) experimental matrix.

Table 4.1. S2 (6 % DVB crosslinked) experimental matrix variables.

S2 (6 % DVB CROSSLINKED) EXPERIMENTAL SERIES			
Experiment Name	Experiment Date	Average Temperature	Average Particle Size, Poly Dispersity
Fe ₂ O ₃ -S2 #1	24- March 1997	55 C°	< 300 nm, 6
Fe ₂ O ₃ -S2 #2	15- April 1997	59 C°	< 300 nm, 5
Fe ₂ O ₃ -S2 #3	5- May 1997	63 C°	< 300 nm, 5
Fe ₃ O ₄ -S2 #1	6- March 1997	55 C°	> 1100 nm, 7
Fe ₃ O ₄ -S2 #2	30- April 1997	57 C°	< 1000 nm, 7
Mixed Oxides	21- April 1997	59 C°	< 500 nm, 5

Average particle size determination and poly dispersity readings (PD) were obtained from a nanosizer in addition to a visual microscopic inspection. Average particle size determination method was summarized in Appendix C.

The total amount of exposed iron (325000 µgrams) was calculated by measuring flow rate over the mixed bed at different times of an experimental run. Average resistivity measurement from the top of the bed and bottom of the bed was 12 MΩ-cm. This particular hematite powder obtained from Verbatim had the smallest particle size (200-300) nm among the other iron oxide powders used. Particle size distribution data from all iron oxide powders are presented in the Appendix C.

Two types of iron uptake were observed by cation exchange resins. The first form of iron, surface iron, was removed by sonicating the cation resins 99 minutes in 100 ml nanopure water using a Branson ultrasonic cleaner. The cleaner had a working volume of 2.25 gallons and had 65.8 Watts of power. The 99 minute sonication cycle was repeated with 100 ml fresh nanopure water until 1 % of the first solution concentration was obtained. Concentrations of the sonicated solutions were determined by UV/Vis

spectrophotometer at 508 nm. Time versus accumulated amount of iron were plotted until a flat line (plateau) was achieved then sonication was terminated. When the sonication was terminated, color of the sonicated cation resins looked very clean, as if they were taken from an original sample bottle. Table 4.2 is a representation of the surface iron data obtained from Fe₂O₃-S2 #3 run. Figure 4.1 shows the data from Fe₂O₃-S2 #3 run as accumulated amount of iron versus sonication time.

Table 4.2. The surface iron data, Fe₂O₃-S2 #3.

# of Washes	Sonication time min	Average concentration μ gram/ml	Accumulated iron μ gram/gr
SW1	99	32.145	2924.940
SW2	198	11.045	3929.936
SW3	297	8.925	4742.038
SW4	396	5.622	4977.337
SW5	495	0	4977.337

* SW # refers to standard water wash to remove surface iron.

* AW # refers to acid wash to remove matrix diffused iron.

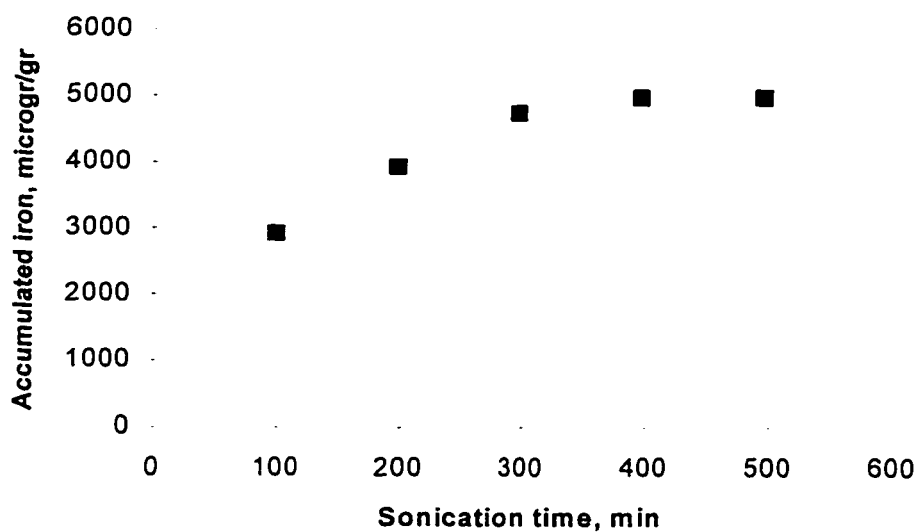


Figure 4.1. Surface iron plateau, Fe₂O₃-S2 #3.

Figure 4.2 is a representation of the exponential fit curve for the accumulated amount of surface iron from Fe₂O₃-S2 #3 run. Since the detection limit of iron using a HP 8452 Diode Array Spectrophotometer was 1 µgram/ml, the error was expected for the low concentration readings. Therefore an exponential fit curve was created estimating the total amount of accumulated iron including the part that could not be detected in the experiments due to the detection limit of the spectrophotometer. The exponential fit curve intercepts the y-axis at 5877.74 µgrams/gr. However, the experimental value for the total amount of accumulated iron is 4977.33 µgrams/gr. All the bar graphs and discussions presented here use the experimental values and not the exponential fit curve data.

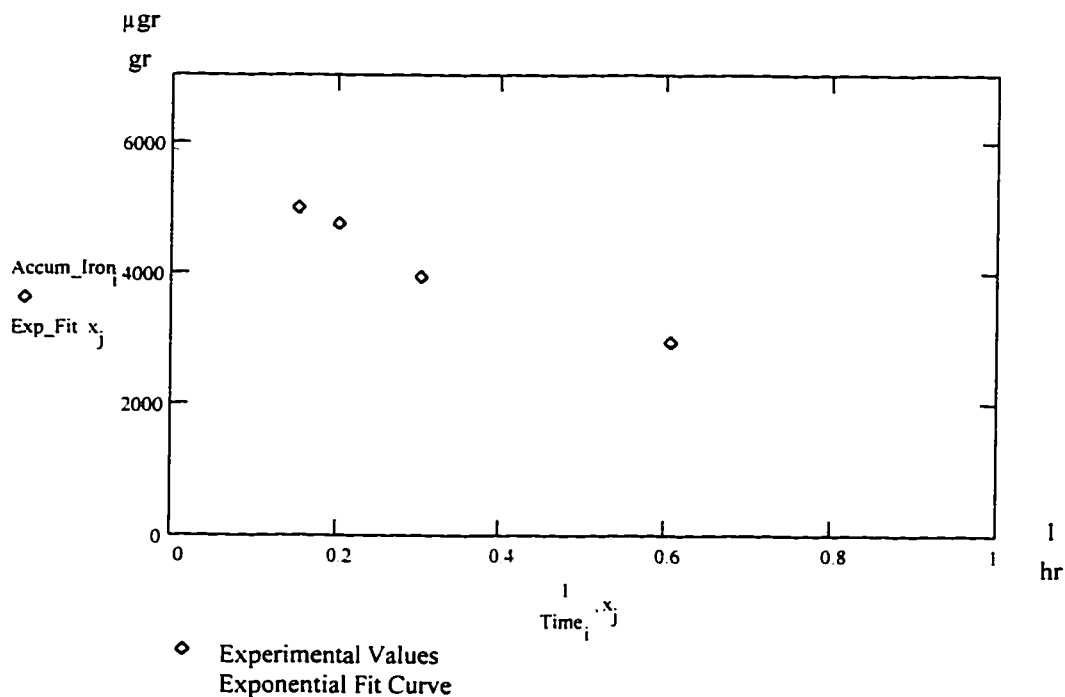


Figure 4.2. Exponential fit curve for the amount of surface iron, Fe₂O₃-S2 #3.

The second form of iron, matrix diffused iron, was removed by sonicating the cation resins in 15 ml 6N H₂SO₄ acid using the Branson ultrasonic cleaner. The cleaner water temperature was set up at 55 C° in order to heat up the acid. Ninety-nine (99) minute sonication cycles were repeated with 15 ml fresh acid. Concentrations of the sonicated acid solutions were determined by UV/Vis spectrophotometer at 508 nm. Table 4.3 shows the amount of acid extracted iron data from Fe₂O₃-S2 #3 experimental run. Time versus accumulated amount of iron are plotted in Figure 4.3.

Table 4.3. The matrix diffused iron data, Fe₂O₃-S2 #3.

# of Washes	Sonic time min	Average concentration μ gram/ml	Accumulated iron, μ gram/gr.
AW1	99	80.966	1101.073
AW2	198	15.054	1305.794
AW3	297	3.667	1355.664
AW4	396	0	1355.664

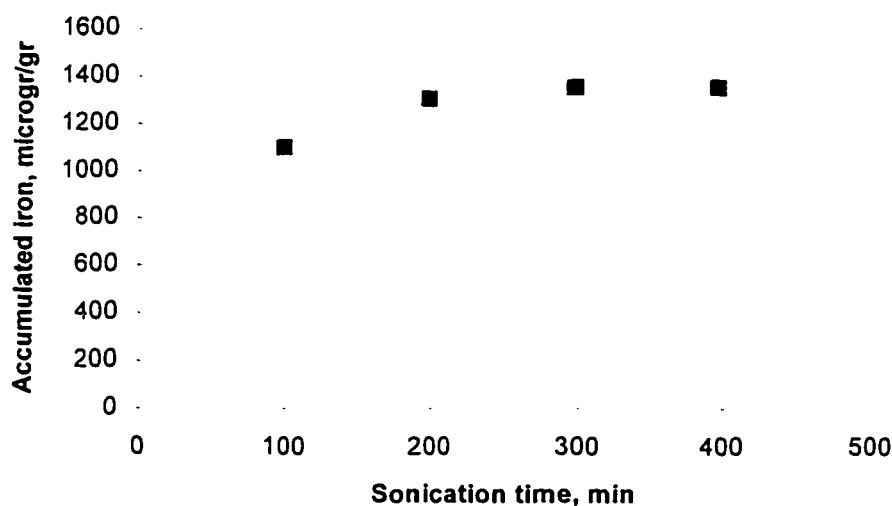


Figure 4.3. Matrix diffused iron plateau, Fe₂O₃-S2 #3.

Figure 4.4 presents the error associated with the amount of accumulated matrix bound iron analysis. An exponential fit curve was created estimating the total amount of accumulated iron including the part that could not be detected in the experiments due to the detection limit of the spectrophotometer. The exponential fit curve intersects the y-axes at 1517.641 $\mu\text{grams/gr.}$, which is the estimated total amount of accumulated iron. On the other hand the amount of accumulated iron that could be measured by the experiment is 1355.66 $\mu\text{grams/}$.

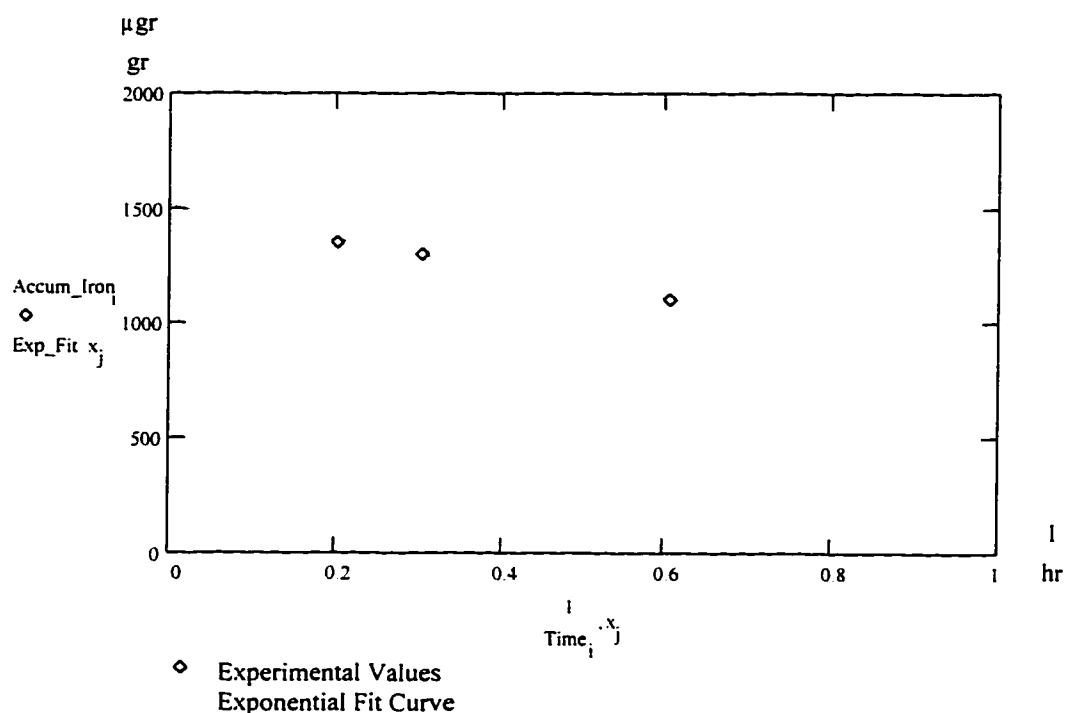


Figure 4.4. Exponential fit curve for the amount of accumulated matrix diffused iron $\text{Fe}_2\text{O}_3\text{-S2 \#3}$.

The data showing total amount of surface iron and matrix diffused iron from the Fe₂O₃-S2 #1, Fe₂O₃-S2 #2, Fe₂O₃-S2 #3 and Fe₃O₄-S2 #2 experimental runs are listed in Table 4.4 and presented in Figure 4.5.

Table 4.4. S2 Experimental matrix data.

Sample Name	Surface Iron, (SI) μgram/gr.	Matrix Diffused Iron, (MDI) μgram/gr.	Total Iron Exposure, (TIE) mg.	% MDI / TIE	% MDI / SI
Fe ₂ O ₃ -S2 #1	3629.20	514.550	272981	0.190	14.2
Fe ₂ O ₃ -S2 #2	3443.56	833.880	310000	0.270	24.2
Fe ₂ O ₃ -S2 #3	4977.33	1355.66	325000	0.420	27.2
Fe ₃ O ₄ -S2 #2	5485.02	488.247	250000	0.195	8.9

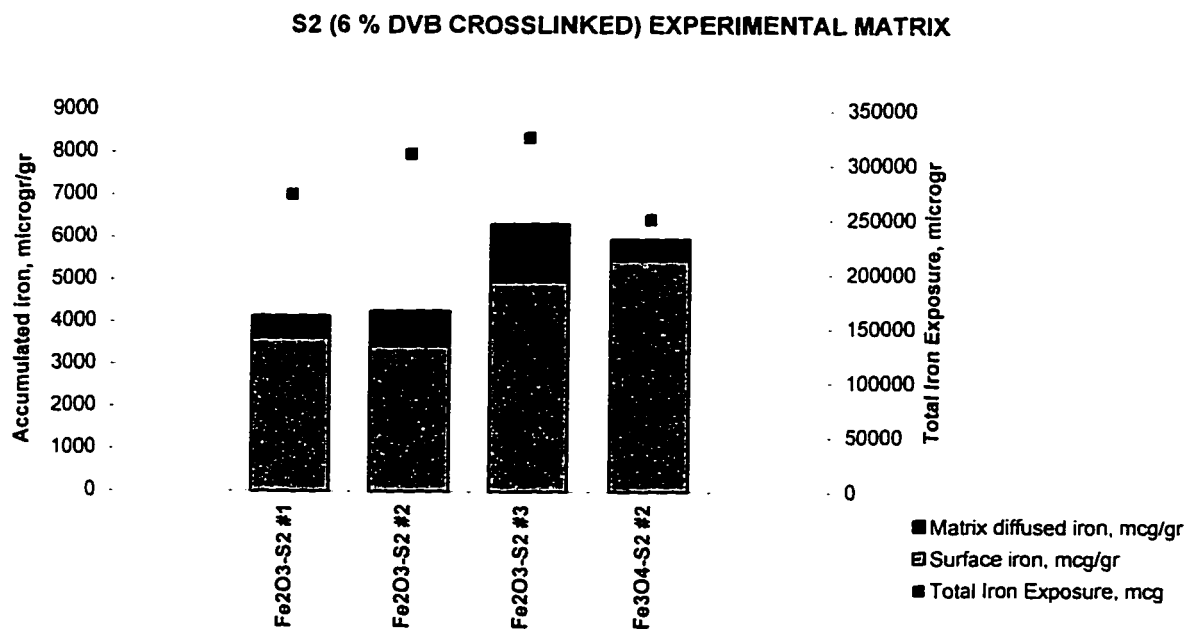


Figure 4.5. Accumulated amount of iron and total iron exposure, S2 matrix.

4.2.1. Fe_2O_3 Runs With S2

Hematite runs with S2 sample were performed three times. The amount of both the surface iron and the matrix diffused iron increased, even though, the total iron exposure was kept within a relatively narrow range.

Two factors contributing to the variations of the data obtained in those experimental runs are listed below.

1. Daily recorded temperature data showed three different average temperature values for Fe_2O_3 -S2 #1, Fe_2O_3 -S2 #2, Fe_2O_3 -S2 #3. The average temperature values were 55°C , 59°C , and 63°C , respectively. Since high temperature and lower particle size increase the exchange rate, this explains the increase of diffused matrix iron from an initial value of $514.55 \mu\text{grams/gr.}$ at 55°C to $1355.66 \mu\text{grams/gr.}$ at 63°C .
2. Iron solutions were sonicated in order to keep the iron particles suspended in the solution. Thus the frequency of sonication (which could not be performed during night time) affected the concentration of the iron solution that was fed to the mixed bed.

4.2.2. Fe_3O_4 Runs With S2

Two experiments were performed using Fe_3O_4 solution with S2 sample. Fe_3O_4 -S2 #1 run performed on March 6, 1997 showed less amount of surface and matrix diffused iron than Fe_3O_4 -S2 #2 run. Daily observations showed that particle size distribution of the Fe_3O_4 -S2 #1 solution was $1\text{-}1.5 \mu\text{m}$. The average pore size of the cation exchange resins is $0.7\text{-}0.8 \mu\text{m}$; therefore, particles larger than this size could not pass through the pores. As a result less amount of surface iron accumulation was observed on this particular run.

The cation resins used in Fe₃O₄-S2 #1 experimental run were sonicated with 6N cold acid (H₂SO₄) rather than hot acid. However, all the other acid wash sonications in S2 and H1 experimental matrixes were done in hot acid. Therefore, less amount of matrix diffused iron was detected in this particular run. The data obtained from Fe₃O₄-S2 #1 experimental run is not included in the tables.

4.2.3. Mixed Oxide Run With S2

One experimental run was performed on April 21, 1997 using four different oxide sources with different weight percentages that are listed in Table 4.5. Work by Hermansson *et al.* (1993) presented the weight percentage of the 4 common iron oxide phases in Swedish Power Plant's Condensate Polishers. X-ray diffraction and scanning electron microscopy were used while determining the phases by Hermansson *et al.* (1993). However, Sawicki *et al.* (1994) reported that weight percentages in Table 4.5 given by Hermansson *et al.* (1993) eliminated the amorphous phase which can be detected only by Mossbauer spectroscopy. The relative content of different phases along the bed found by Sawicki *et al.* (1994) were (%55) Fe₃O₄, (%15-20) γ -FeO(OH), (%20-15) α -FeO(OH), (%10) Fe₂O₃. In future studies, the weight percentages given by Sawicki *et al.* (1994) have to be used.

Table 4.5. Mixed oxide weight percentages.

Common Phases and Weight Percentages			
Magnetite, Fe ₃ O ₄ -% 55	Hematite, Fe ₂ O ₃ -% 15	Goethite, α-FeO(OH) -% 15	Lepidocrocite, γ- FeO(OH) -% 15

The mixed oxide experimental run showed lower amount of total iron exposure than the Fe₂O₃ runs performed with the same cation exchange resins. Daily observations showed that low amount of iron exposure on the mixed bed caused by rapid tubing abrasion on the master flex pump created concentration variations. Table 4.6 shows the data obtained from the mixed oxide experiment. Figure 4.6 is a representation of the data in Table 4.6 as accumulated amount of iron versus total iron exposure.

Table 4.6. Mixed oxide data, S2 .

Sample Name	Surface Iron, (SI) μgram/gr.	Matrix Diffused Iron, (MDI) μgram/gr.	Total Iron Exposure, (TIE) mg/gr.	% MDI / TIE	% MDI /SI
Mixed Oxides	1754.01	642.55	119059.20	0.54	36.63

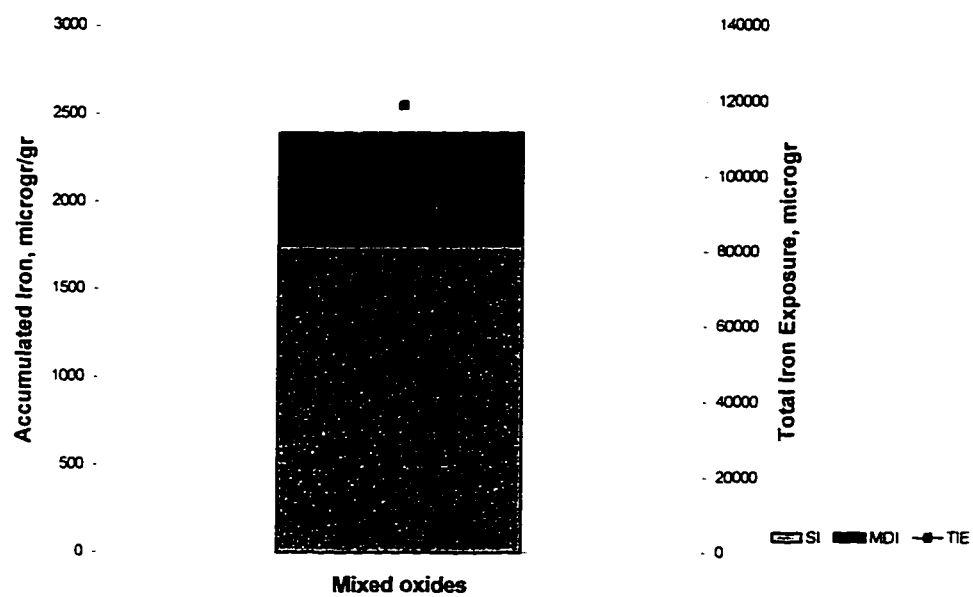


Figure 4.6. Accumulated amount of iron and total iron exposure, mixed oxides.

4.3. H1 (10 % DVB CROSSLINKED) EXPERIMENTAL MATRIX

Table 4.7. H1 (10 % DVB crosslinked) experimental matrix variables.

H1 (10 % DVB CROSSLINKED) EXPERIMENTAL SERIES			
Solution name	Experiment Date	Average Temperature	Average Particle Size, Poly Dispersity
Fe ₂ O ₃ -H1 #1	10-May 1997	63 C°	< 300 nm, 6
Fe ₃ O ₄ -H1 #1	16-May 1997	63 C°	< 900 nm, 5

Table 4.7 is a representation of the experimental temperature, average particle size of the oxide solutions and poly dispersity of the oxide solutions over the experimental runs.

Since H1 (10 % DVB crosslinked) is a standard cation exchange resin most commonly used in deep bed condensate polishers, it was chosen as a comparison medium to S2 (6% DVB crosslinked) sample. Having a 10 % DVB crosslink, H1 has less porous (open) polymeric matrix structure than S2. Therefore, amount of iron uptake by H1 sample is expected to be much less than that of S2 (6%) sample.

Combined data from H1 (10 %) sample are listed in Table 4.8. Due to time constraint only hematite and magnetite solutions in the H1 Experimental Matrix were run.

Table 4.8. H1 Experimental matrix data.

Solution name	Surface Iron, (SI) μ gram/gr.	Matrix Diffused Iron, (MDI) μ gram /gr.	Total Iron Exposure, (TIE) μ gram	% MDI / TIE	% MDI / SI
Fe ₂ O ₃ -H1 #1	3353.6	280.2	305000	0.092	8.36
Fe ₃ O ₄ -H1 #1	4790.3	213.1	310005	0.069	4.45

Figure 4.7 is a representation of the data in Table 4.8 as accumulated amount of iron versus total iron exposure on Fe_2O_3 -H1 #1 and Fe_3O_4 -H1 #1 runs.

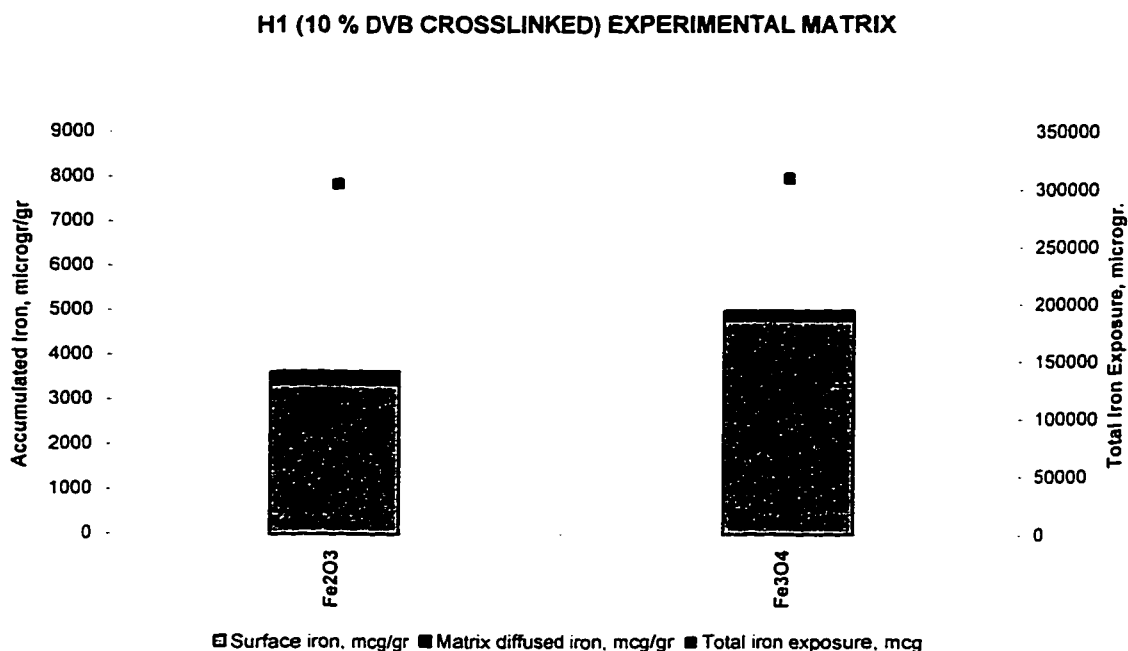


Figure 4.7. Accumulated amount of iron and total iron exposure, H1 matrix.

4.4. Saturated Amount of Ferric ion Loading on S2 and H1

Saturated amounts of ferric ion were loaded onto the cation exchange resins using ferric chloride hexahydrate, $\text{FeCl}_3 \cdot 6\text{H}_2\text{O}$, solution. Determination method was developed by Dr. Leon Yengoyan and saturated amount of ferric ion analysis was performed by Mary Silva. The amount of ferric ion into the cation exchange resins at the saturation level is described in Appendix B. Cation exchange resins, at the saturation levels, loaded with ferric ion are presented in Table 4.9.

Table 4.9. Fe³⁺ Saturation Data.

Sample Name	Amount of Bound Fe ³⁺ , mg/gr.
H1 (10 % DVB)	96.80
S2 (6 % DVB)	110.66

In the experimental runs, particulate iron oxide solutions were fed onto the cation exchange resins and were expected to dissolve in the vicinity of the sulfonate groups acting as a presumed acidic environment at a pH of 3. However, in FeCL₃.6H₂O solution, iron was already in the form of Fe³⁺ ion. That is why the numbers in Table 4.9 are much higher than the numbers obtained in the experimental runs.

CHAPTER 5. DISCUSSION

The purpose of this study was to identify the form of iron uptake by cation exchange resins. One sample with a higher crosslink density (10 % DVB, H1) and one with a lower crosslink density (6 % DVB, S2) were used. In this section, values of the experimental data from both S2 sample and H1 sample are combined together and summarized below. Table 5.1 lists normalized values of the experimental data obtained from S2 sample runs.

Table 5.1. Percentage of MDI over TIE, SI; S2.

Oxide Solutions	% MDI / TIE	% MDI / SI
Fe ₂ O ₃ -S2 #1	0.19	14.2
Fe ₂ O ₃ -S2 #2	0.27	24.2
Fe ₂ O ₃ -S2 #3	0.42	27.2
Fe ₃ O ₄ -S2 #2	0.195	8.9

- * Matrix Diffused Iron, MDI
- * Total Iron Exposure, TIE
- * Surface Iron, SI

Figure 5.1 and 5.2 are representations of the data from S2 sample in Table 5.1. The average value of matrix diffused iron over total iron exposure is 0.27 % in the four experimental runs performed using S2 sample. The average value of matrix diffused iron over surface iron is 18.635 %.

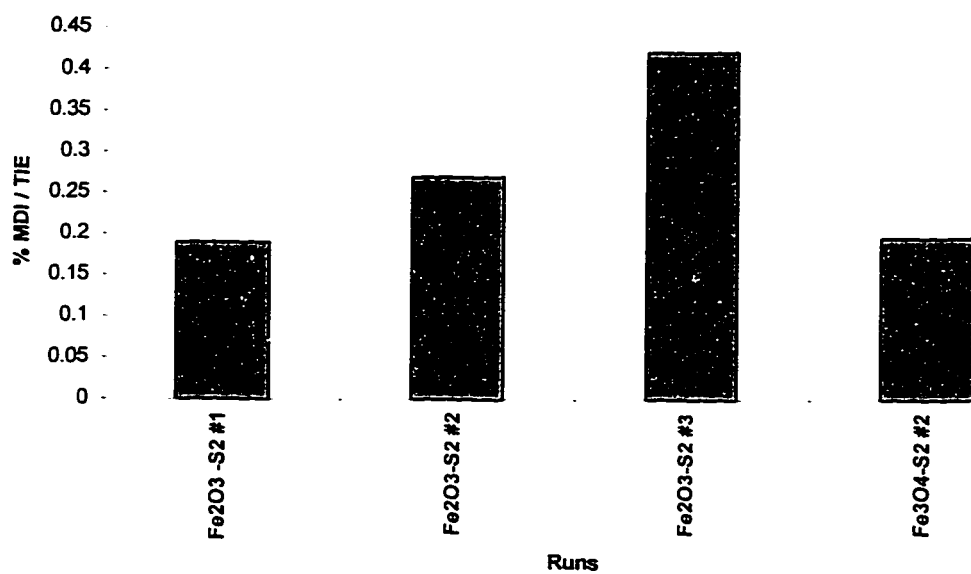


Figure 5.1. % Matrix diffused iron over total iron exposure, S2.

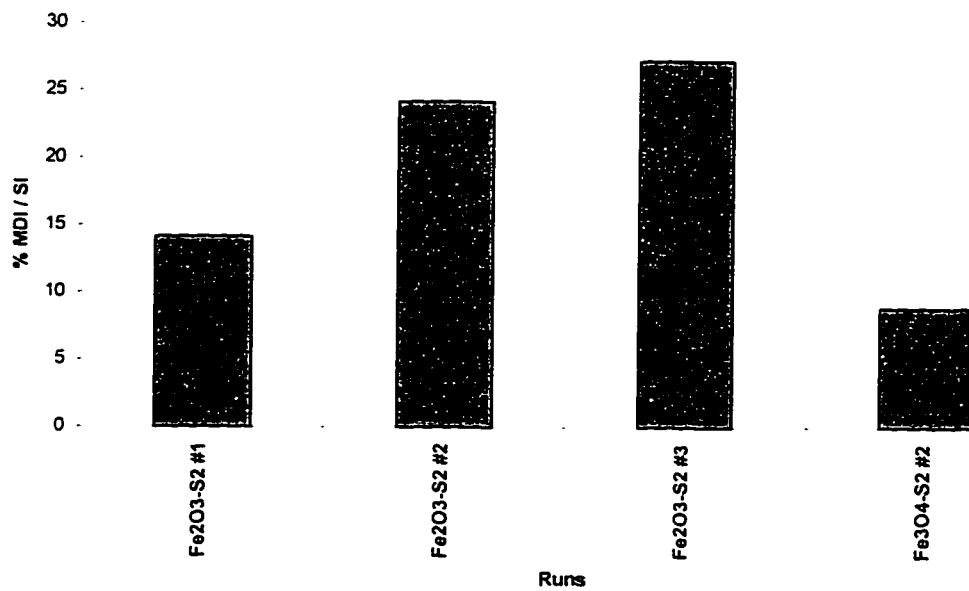


Figure 5.2. % Matrix diffused iron over surface iron, S2

Table 5.2. Percentage of MDI over TIE. SI; H1

Solution name	% MDI / TIE	% MDI / SI
Fe ₂ O ₃ -H1 #1	0.092	8.355
Fe ₃ O ₄ -H1 #1	0.069	4.450

* Matrix Diffused Iron, MDI

* Total Iron Exposure, TIE

* Surface Iron, SI

Figure 5.3 and 5.4 are representations of the data from H1 sample in Table 5.2.

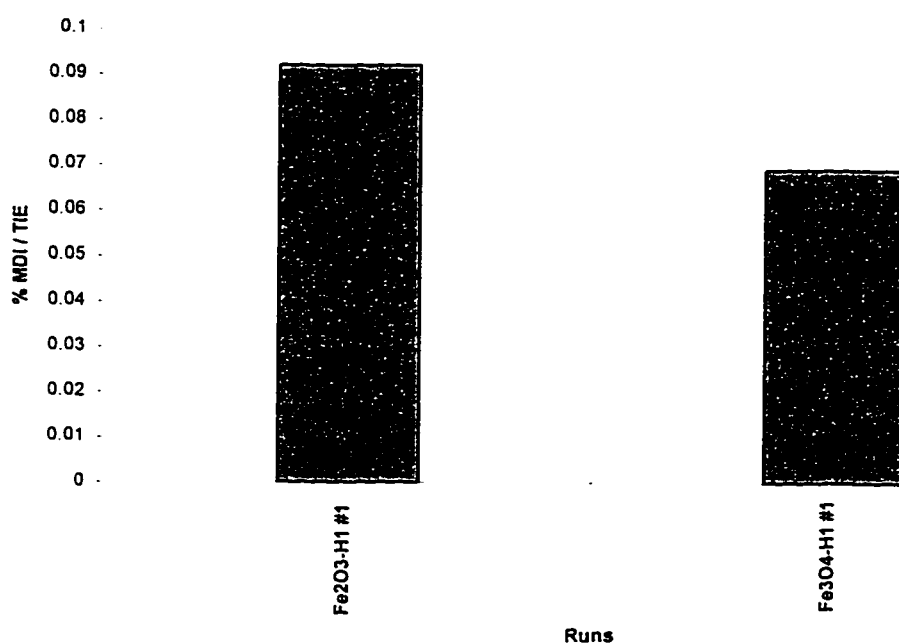


Figure 5.3. % Matrix diffused iron over total iron exposure, H1

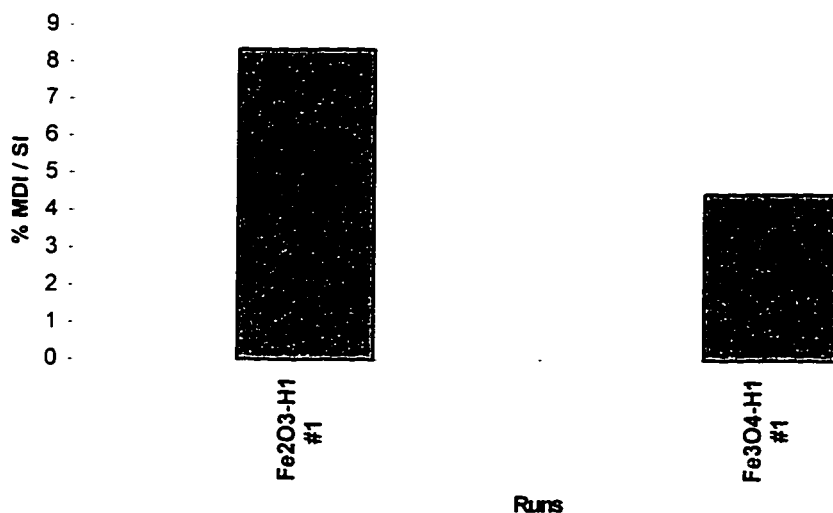


Figure 5.4. % matrix diffused iron over surface iron, H1.

The average value of matrix diffused iron over total iron exposure is 0.08 % in the two experimental runs performed using H1 sample. The average value of matrix diffused iron over surface iron is 6.4 %.

A comparison of the data in Figures 5.1 and 5.3 shows approximately three times higher amount of matrix diffused iron over total iron exposure for the S2 (6 % DVB crosslinked) cation resins than for the H1 (10 % DVB crosslinked) cation resins.

The percentage of matrix diffused iron over surface iron is similarly three times higher for the S2 (6 % DVB crosslinked) cation resins than for the H1 (10 % DVB crosslinked) cation resins. Since higher percentage of crosslink curtails the swelling and amount of water retention, causing more brittle polymeric matrices, reduced amount of iron uptake by H1 sample was expected.

For a better comparison, Fe_2O_3 runs in Figure 5.5. and Fe_3O_4 runs in Figure 5.6. are presented separately.

Table 5.3. Percentage of MDI over SI; S2 and H1 .

Solution name	% MDI / SI	Average Solution Temperature, °C
Fe_2O_3 -H1 #1	8.4	63
Fe_2O_3 -S2 #1	14.2	55
Fe_2O_3 -S2 #2	24.2	59
Fe_2O_3 -S2 #3	27.2	63
Fe_3O_4 -H1 #1	4.5	63
Fe_3O_4 -S2 #2	8.9	57

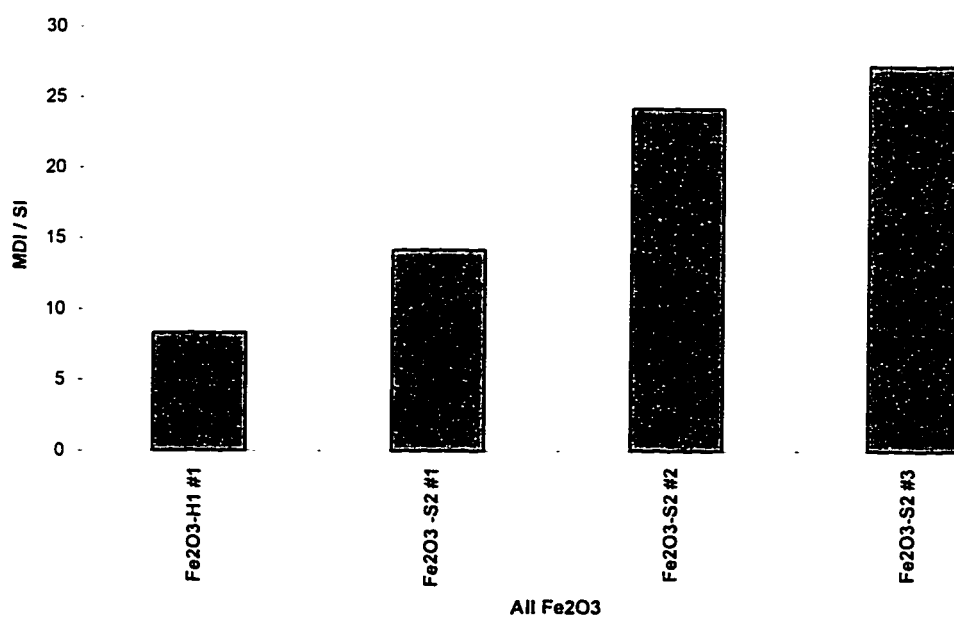


Figure 5.5. % Matrix diffused iron over surface iron, all Fe_2O_3 runs

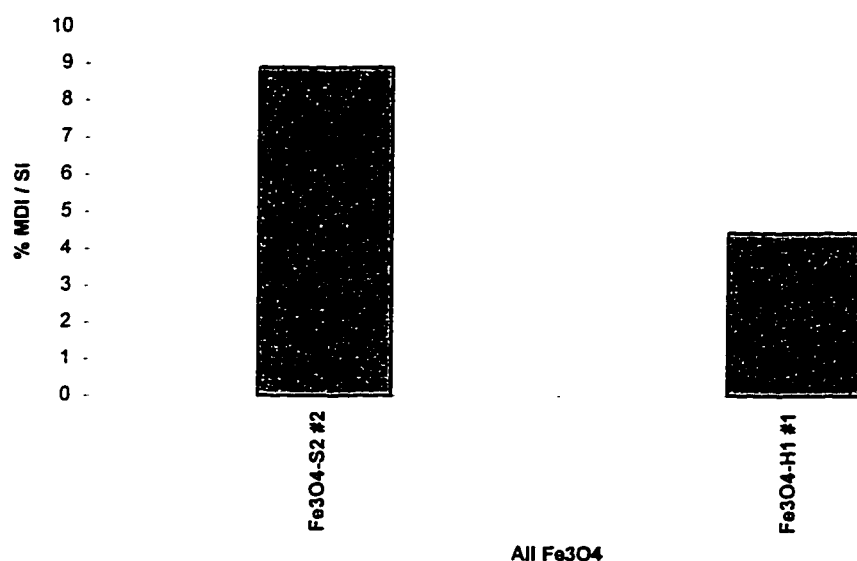


Figure 5.6. Matrix diffused iron over surface iron for all Fe_3O_4 runs

The average of the MDI / SI (matrix diffused iron over surface iron) percentages for the Fe_2O_3 runs is approximately three times higher than the average for the Fe_3O_4 runs. Higher temperature and lower particle size enhanced the rate of exchange in the Fe_2O_3 runs.

Diffusion kinetics involved in this study may be divided into three steps: mass transfer in the external solution up to the surface of the resin particles (film diffusion), diffusion inside the resin phase (particle diffusion), and chemical exchange in the vicinity of the exchange groups. Difficulties in mass transfer from the external solution to the surface of the resin can primarily be seen in the Fe_3O_4 -H1 #1. Since this run had the largest particle size distribution among all the runs, the MDI / SI is lower than all other runs. On the other hand, higher amount of matrix diffused iron obtained from Fe_2O_3 runs

shows an agreement with the diffusion kinetics due to the fact that all the Fe_2O_3 runs had small particle sizes and higher temperature distribution over the mixed bed.

The iron determination methodology applied in this study relates to the study done by Yushikawa *et al.* (1989). Yushikawa *et al.* (1989) hypothesized that lower pH range in the pores of a cation exchange resin would produce soluble iron with a chemical bond between Fe^{3+} and SO_3^- . Yushikawa *et al.* (1989) also emphasized that this ferric ion would only be removed by HCL or H_2SO_4 acid. Yushikawa *et al.* (1989) called this iron incorporated iron, which is called matrix diffused iron in this study and is removed by an acid extraction as Yushikawa *et al.* (1989) suggested. This could be the chemistry, in the pores of the cation exchange resins, between Fe^{3+} and SO_3^- .

Crud removal results reported by Yushikawa *et al.* (1989) are listed in Table 5.4. The sum of loosely captured and tightly captured iron is called surface iron in this study. Table 5.4 shows higher amount of matrix diffused iron to surface iron ratio then obtained in this study. However, Yushikawa *et al.* (1989) does not report the pH range of the solution entering the mixed bed. If the pH range is between 3.5 and 4, iron solution will become soluble before it enters the mixed bed and a higher amount of matrix diffused iron will be obtained. In this study all the iron was in the form of particulate iron and the resistivity probes placed at the top and the bottom of the mixed bed showed 12 $\text{M}\Omega\text{-cm}$ resistivity. As a result, dissolution of the iron did not take place before the solution entered the mixed bed. Therefore, lower amount matrix diffused iron compared to the one reported by Yushikawa *et al.* (1989) was expected.

Table 5.4. Crud removal results reported by Yushikawa *et al.* (1989)

Form of Iron	Conventional Cation, (10 % DVB)	Low Crosslink, (6 % DVB)
Loosely Captured	0.57 gr.	0.731 gr.
Tightly Captured	0.007 gr.	0.035 gr.
Incorporated	0.27 gr.	1.3 gr.

CHAPTER 6. CONCLUSION

Styrene based divinyl-benzene (DVB) crosslinked and strongly sulfonated cation exchange resins investigated in this study have been successful in producing matrix diffused iron. All seven experimental runs resulted in generating matrix diffused iron over 120 hours of an experimental run.

The results of the experiments showed that the percentage of both MDI / TIE (matrix diffused iron over total iron exposure) and MDI / SI (matrix diffused iron over surface iron) for the S2 (6 % DVB crosslinked) cation resins were approximately three times higher than for the H1 (10 % DVB crosslinked) cation resins.

Further studies are required to determine whether matrix diffused iron is derived from local dissolution in the resin pores of surface iron oxides and should also seek repeatability and reproducibility in the experimental series performed in this study so that error free comparison between the lowest and the highest crosslinked cation exchange resin can be done. Flow loop used in this study should be updated with a better temperature control and more uniform particle size distribution.

Future experiments should be done using 2:1 (anion: cation) ratio instead of 1:1 ratio, since the exchange capacity of the anion resins are lower than the exchange capacity of cation resins. Reported weight percentage values for iron oxide phases by Sawicki *et al.* (1994) should be used for further investigations.

REFERENCES

- Yoshikawa, S., 1989, 50th Anniversary Meeting International Water Conference, *Electric Power Company*, Tokyo, Japan, October 23-25.
- Hermansson, H. P., 1994, Factors Influencing the Precoat Filtration of Boiling Water Reactors Water Stream, *Nuclear Technology*, Vol. 108, Oct.
- Hermansson, H. P. and Persson, G., 1989, Precoat Filter Studies in BWRs, Water Chemistry of Nuclear Reactor Systems 5, *British Nuclear Energy Society*, London.
- Ishigure, K., Takahashi, M. and Wagoya, Y., 1983, Adsorption of Model Crud on Ion Exchange Resins, *Industrial Research Institute*, Tokyo, Water Chemistry 3. BNES, London.
- Takahashi, M. and Ishigure, K., 1987, Kinetics of Filtration of Model Crud with Ion Exchange Resin Bed, *Nuclear Science and Engineering*, Vol. 97, 211-219.
- Lundgrun, K., 1980, Transport of Corrosion Products in a BWR, *Water Chemistry II*, BNES, 45.
- Suslick, K. S., Fang, M. and Hyeon, T., 1996, Sonochemical Synthesis of Iron Colloids, *Journal of American Chemical Society*, Vol. 118, 11960-11961.
- Cao, X., Koltypin, Y. and Kataby, G., 1995, Controlling The Particle Size of Amorphous Iron Nanoparticles, *Journal of Material Research Society*, Vol. 10-11, Nov.
- Rajagopalan, R. and Chu, R. Q., 1982, Dynamics of Adsorption of Colloidal Particles in Packed Beds, *Journal of Colloid and Interface Science*, Vol. 86, No. 2, April.
- Public Service Electric and Gas Co., 1993, BWR Condensate Filtration Studies, *EPRI TR-102929 Project 3388 Interim Report*, Sep.
- Ishigure, K., 1987, Kinetics of Filtration of Model Crud with Ion Exchange Resin Bed, *Nuclear Science and Engineering*, Vol. 97, 211-219.
- Ishigure, K., Takahashi, M. and Kawaguchi, M., 1983, Adsorption of Model Crud on Ion Exchange Resin Beads, *Water Chemistry 3. BNES*, London.
- Kimura, K., 1991, Magnetic Properties of Iron: From Clusters to Bulk, *Physics Letters A*, Vol. 158, 85-88.

Suslick, K. S., 1995, Applications of Ultrasound to Materials Chemistry, *Journal of Materials Education*, Vol. 17, 185-201.

Pourbaix, M., 1966, Atlas of Electrochemical Equilibria in Aqueous Solutions, *Pergamon Press*, New York.

APPENDICES

Appendix A: UV/VIS Spectrophotometer

Concentration measurements were based on the absorbance of iron containing solutions which are proportional to their concentration. This determination was performed with a HP 8452 Diode Array Spectrophotometer, HP 89530 MS-DO UV/VIS Software Handbook at 508 nm.

In the HP 8452A Diode Array Spectrophotometer a single collimated beam of light is passed through the sample before being dispersed onto the diode array. This allows simultaneous access to all wavelength information. The result is a fundamental increase in the rate at which data can be acquired.

A single-component quantitation analysis with an HP 8452 spectrophotometer and MS-DOS UV/ VIS software consists of three main steps.

1. Setting measurement parameters.(Analytical and reference wavelength, calibration curve)

Analytical Wavelength: The analytical wavelength is the wavelength we have chosen to make our absorbance measurements. A single or a wavelength range can be used for quantitation. We have chosen a single wavelength at 508 nm.

Reference Wavelength: The absorbance at the reference wavelength is subtracted from the absorbance at the analytical wavelength. This absorbance is used for quantitation. Reference wavelength can also be used to improve precision by minimizing solution noise due to dust particles or air bubbles or drift in lamp intensity.

2. Determining the calibration curve: The type of calibration curve was selected to determine concentrations. The best curve to use dependent upon the samples, the dynamic range over which we were measuring the deviations from Beer's Law.

Once the measurements were set , the next step was to develop the calibration curve. This was done by scanning a series of standard solutions of known concentration (μml). By measuring their absorbance at the appropriate wavelength, we had created a calibration curve of absorbance versus concentration for the analytical/ reference wavelength.

3. After the standards were scanned, solutions with unknown concentrations were scanned to determine their concentration.

Appendix B: Fe³⁺ Determination Method

Fe³⁺ determination methodology was originally developed by Dr. Leon Yengoyan in Chemistry Department and by Dr. Paul Frattini from EPRI.

Ferric (Fe³⁺) Ion Loading On Cation Exchange Resins:

To determine saturation amount of iron to the cation exchange resins, One gram of the resin was placed on a chromatography column and washed with 200 mM ferric chloride solution (54 grams of ferric chloride hexahydrated (FeCl₃.6H₂O in 1000 ml of nanopure water). The total wash solution was 300 ml. The iron treated resin was washed with deionized water until unbounded iron was removed. This was determined by analysis of the wash solution. The sample was kept under vacuum for dry weight base.

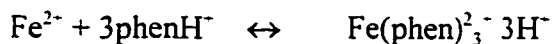
Ferric Ion Removal On Cation Exchange Resins:

- One gram of the dry cation exchange resins were weighted.
- Cation exchange resins were placed in a chromatography column and washed at a rate of 100 ml/30 min. with 6N H₂SO₄ acid. Every 100 ml of washed acid sequentially were collected. One (1.0) ml of this solution was placed in a 100 ml volumetric flask. One (1.0) ml of hydroxylamine hydrochloride (10 grams of H₂NOH.HCL is dissolved in about 100 ml of deionized water), 10 ml of sodium acetate (166 grams of NaOAc.3H₂O is dissolved in 1000 ml of deionized water) and 10 ml of orthophenantroline solution (0.1 grams of orthophenantroline monohydrate is dissolved in 100 ml deionized water) were also added to the 100 ml volumetric flask and diluted to 100 ml mark. First the standards then the iron containing solutions were run through the spectrophotometer.

Preparation of the Standards for Calibration Curve

- Standard iron solution 70.2 grams of reagent-grade $\text{Fe}(\text{NH}_4)_2(\text{SO}_4)_6 \cdot \text{H}_2\text{O}$ was dissolved into a 1-liter volumetric flask containing 1 to 2 ml of concentrated sulfuric acid and diluted to the mark.

The red-orange complex that forms between iron(II) and 1, 10-orthophenanthroline is useful for determining iron in water supplies. The reagent is a weak base that reacts to form phenanthroline ion, phenH^+ , in acidic media. Complex formation with iron is thus best described by the equation



The formation constant of this equilibrium is 2.5×10^6 at 25°C . Iron(II) is quantitatively complexed in the pH range between 3 and 9. A pH of about 3.5 is ordinarily recommended to prevent precipitation of iron salts, such as phosphates.

An excess of a reducing agent, such as hydroxylamine or hydroquinone, is needed to maintain iron in the +2 state. The complex, once formed, is stable.

Appendix C: Preparation of An Iron Oxide Solution Suspension:

The purpose in the preparation of an iron oxide solution is to achieve optimum operation condition for ion exchange phenomenon which includes several factors such as concentration of solution in contact with the resin, stirring or mixing rate, diameter of resin particle, size of ions and diffusion rate of the ions involved.

Iron oxide particle size plays an important role in the uptake performances of the ion exchange resins. If the ions coming from the bulk solution are larger than the size of the pores, diffusion to the inside of the resins would not happen. If they are not then the expected particle diffusion would happen and chemical exchange in the vicinity of the exchange groups will occur. Same fundamentals applies to the iron oxide particles approaching to the pores. Certain particle size limitations have to be established for the optimum performance.

From previous studies conducted in Swedish and American power plants showed that % 75 corrosion product particles released to the feed water had particle sizes ranging between 0.1-1 μ m.

All four types of iron oxide powders purchased from Alfa Aesar have different particle sizes ranging 5-10 μ m. However, styrene divinyl-benzene crosslinked cation exchange resins have pore sizes in the range of 0.4- 0.5 μ . To achieve the optimum diffusion rates, and to create same particle size exposure to the beads as it happens in the real plants, iron powder particle size needs to be reduced.

Two different particle size reduction methods were applied.

- Each oxide sample pounded for 15 min.(%0.005 by weight), then nanosizer were used for particle determination and visual inspection with a microscope.
- Each oxide sample pounded for 15 min. on % 0.0125 by weight, then nanosizer were used for particle determination and visual inspection with a microscope.

It showed that weight percentage played an important role when lowering the particle size. Samples prepared with lower weight percentage showed much closer particle size ranges than the samples prepared with the higher weight percentage. Weight reduction made sonication easier for the solution. Particularly, hematite powders obtained from Verbatim had much smaller known particle sizes (200 nm). Solutions prepared with this particular sample showed uniform suspensions for longer period of time (exp. over night). Particle size distribution of the solutions are listed with the poly dispersity data in the table below.

Type of oxide	Weight % .005	Weight %.00125	Mixing over night Sonication continuous only day time
Fe ₃ O ₄	>3000 nm	<2000 nm	< 850 nm, PD 7
Fe ₂ O ₃	>3000 nm	<1000 nm	< 300 nm, PD 6
α-FeO(OH)	>2500 nm	<1500 nm	< 500 nm, PD 6
γ-FeO(OH)	>2000 nm	<1500 nm	< 500 nm, PD 5

Appendix D: Experimental Run Time Calculations

- Iron on to the beads in flow as Magnetite:

$$(150 \text{ ml} / \text{min}) \times (\Delta t \text{ min}) (1 \text{ gr} / \text{ml}) \times (300 \times 10^{-9} \text{ grFe}^3\text{O}^4 / \text{grsol}) \times \frac{3 \times (56)}{3 \times (56) + 4 \times (16)} \times 0.65 \times 0.33 = 6.9896 \times 10^{-6} \times \Delta t (\text{min}) \text{ grams}$$

- Iron required by detection limit of UV-Vis (on full bed):

$$(1 \times 10^{-6}) \text{ gr} / \text{ml} \times 100 \times 300 \text{ ml} / \text{grbeads} \times [\Pi \times (1^2) \times (2) \text{ cm}^3] \times (1.3 \text{ gr} / \text{cm}^3) \times (0.6) \times \left(\frac{1}{2}\right) = 8.6 \times 10^{-2} \text{ grams}$$

- Run time at limit of detection:

$$\Delta t (\text{min}) = \frac{8.6 \times 10^{-2}}{6.9896 \times 10^{-6}} = 12305 \text{ min} = 8.5 \text{ days}$$

- Run time at 5 times detection limit:

$$5 \times 8.5 = 42.75 \text{ days}$$

- Enhancements:

Dilute 100 ml aliquot of acid wash to 1 liter of orthophenanthroline instead of 1 ml to 100 ml. This reduces run time to 4.2 days.

Appendix E: Flow Loop Mass Balance Calculations:

1. The maximum water flow rate through a nanopure system is 19 lt./hr. Since operation variations have an effect on the operation of the system, the expected flow rate is 150 ml/min.

2. Laboratory scale mixed bed dimensions was chosen as 1" in diameter and 1" in depth.

Mass Balance on the crud solution:

First Stream $\rightarrow Q1, H_2O$

Second Stream $\rightarrow Q2, (H_2O + Crud) \Rightarrow \% 0.00125$ (by weight)

Third Stream $\rightarrow 300$ ppb, 150 ml/min. (crud solution)

$$Q1 \times C_{crud} + Q2 \times C_{crud} = 300 ppb \times C$$

$$Q1 \times 0 + Q2 \times \frac{0.00125 \text{ kg crud}}{100 \text{ kg H}_2\text{O}} \times 1000 \frac{\text{kg}}{\text{m}^3} = \frac{300 \text{ kg}}{10^9 \text{ m}^3} \times 150 \frac{\text{ml}}{\text{min}}$$

$$Q2 = 3.6 \frac{\text{ml}}{\text{min}}$$

Flow Regime:

$$150 \frac{\text{ml}}{\text{min}} \times \frac{1}{\pi \times \left(0.5'' \times \frac{2.54 \text{ cm}}{1''} \right)^2} \times 1 \times \frac{1 \text{ min}}{60 \text{ sec}} = 0.5 \frac{\text{cm}}{\text{sec}}$$

$$\text{Re} = \frac{d \times u \times \rho}{\mu} = 2.54 \text{ cm} \times 0.5 \frac{\text{cm}}{\text{sec}} \times 1000 \frac{\text{kg}}{\text{m}^3} \times 1 \frac{\text{m}^2}{10^4 \text{ cm}^2} = 127$$

Pressure Drop On The Packed Bed:

There are N_p spherical ion exchange resins, the solid volume is $N_p \times \Pi \times D_p^3 \div 6$

$$\text{Void Volume: } \frac{\varepsilon}{1-\varepsilon} \times \frac{N_p \times \Pi \times D_p^3}{6}$$

$$\text{Surface Area: } N_p \times \Pi \times D_p^2$$

Ion exchange resins size range is 650-750 μ .

Packed Bed Friction Factor, F_p

Packed Bed Reynolds Number (Re_p)

$$F_p = \frac{D_p \times \varepsilon^3}{\rho \times v_\infty \times (1-\varepsilon)} \times \frac{|\Delta p|}{L}$$

$$F_p = F_p(Re_p)$$

$$Re_p = \frac{D_p \times v_\infty \times \rho}{(1-\varepsilon)^2}$$

$$F_p = \frac{150}{Re_p} + 1.75 = \frac{150}{127} + 1.75 = 2.93$$

$$v_\infty = 0.5 \frac{cm}{sec}$$

$$L = 2.54cm = D_p$$

$$\varepsilon_m = 1 - 0.356 \times (\log D_p' - 1)$$

$$\varepsilon_m = 1 - 0.356 \times (\log 650 - 1) = 0.35$$

$$\Delta p = \frac{F_p \times \rho \times v_\infty \times (1-\varepsilon) \times L}{D_p \times \varepsilon^3}$$

$$\Delta p = \frac{2.93 \times 1000 \frac{kg}{m^3} \times 0.25 \frac{cm^2}{sec^2} \times 0.65 \times 2.54cm}{0.026inch \times \frac{2.54cm}{1"} \times 0.35^3} = 0.427 \frac{kg}{sec^2 \times cm} = 42.7 Pa$$

Appendix F: Power Determination of Branson 5210 Ultrasonic Cleaner

Test Conditions

- Uncovered Bath with support tray in place
- No degas time
- Working Volume = 2.25 gallons
- Temperature Measuring Instruments
 1. Keithley 132 C Multimeter + 1 type K thermocouple
 2. -10 °C to 50 °C thermometer
 3. Built-in Thermometer on Branson 5210 Ultrasonic Cleaner
- Thermocouple and thermometer placed at center of bath, ~ 1 cm above support tray.

Procedure

1. Take Initial Temperature Reading
2. Start Ultrasonic Cleaner
3. Read temperature every 5 minutes

Constants

Density of water = 1 gram/cm³

Heat Capacity of Water = 4.18 kJ/kg*K

Power Calculation

$$Power = (Volumewater) \times (Densitywater) \times (HeatCapacity) \times (ChangeinTemperature) \times \frac{1}{(Operatingtime)}$$

$$V = 8.5 \text{ L}$$

$$\rho = 1 \text{ g/cm}^3$$

$$C_p = 4.18 \text{ kJ/kg} \cdot \text{K}$$

$$\Delta T = 11 \text{ }^\circ\text{C}$$

$$t = 99 \text{ min.}$$

$$Power = 8.5 \text{ L} \times \frac{1 \text{ gr.}}{\text{cm}^3} \times 1000 \frac{\text{cm}^3}{\text{L}} \times 4.18 \frac{\text{kJ}}{\text{kg} \cdot \text{K}} \times 1 \frac{\text{kg}}{1000 \text{ gr}} \times 11^\circ \text{C} \times \frac{1 \text{ K}}{1^\circ \text{C}} \times \frac{1}{99 \text{ min}} \times \frac{1 \text{ min}}{60 \text{ sec}} \times 1000 \frac{\text{J}}{\text{kg.}}$$

$$Power = 65.8 \text{ J/s} = 65.8 \text{ W}$$

Temperature Calibration Data For Branson 5210 Ultrasonic Cleaner

Time, min	On Board thermometer, C	Thermometer, C	Thermocouple meter, C
0	22	22	21
5	23	22	22
10	24	22.5	22
15	24	23.5	23
20	25	24	24
25	25	25	24
30	26	25.5	25
35	26	26	26
40	27	27	26
45	27	27.5	27
50	28	28	28
55	28	28.5	28
60	29	29.5	29
65	30	30	29
70	31	30.5	30
75	31	31	31
80	31	31.5	31
85	32	32	32
90	32	32.5	32
95	33	33	32
99	33	33	32

Temperature Calibration Curve For Branson 5210 Ultrasonic Cleaner

